Magnetization Curve Plotting from the Magnetic Domain Images

H. Endo, S. Hayano, Y. Saito, M. Fujikura, and C. Kaido

Abstract—An innovative image processing methodology is proposed to draw the magnetization curves of electrical steels. Our methodology enables to draw the continuous magnetization curve from a series of the distinct scanning electron microscope (SEM) images of magnetic domains. Our image processing methodology has two distinguished features. One is that the contrast of a domain image is regarded as an average of flux density. Another one is that domain motion observed in several domain images is represented by the image Helmholtz equation. Its solution generates any magnetized states of the magnetic domains. Moreover, computing averaged contrast of each image gives value of flux density on a magnetization curve. In this paper, we apply our methodology to the domain images of a grain-oriented electrical steel. This paper demonstrates the macroscopic- as well as microscopic-magnetization curves reflecting on their physical conditions.

Index Terms—Grain-oriented electrical steel, image processing, magnetic domains, magnetization curve, scanning electron microscope.

I. INTRODUCTION

DYNAMIC observation of magnetic domain have been investigated to clarify the mechanism of magnetization processes [1], [2]. In case of electrical steels, it is also essential to estimate iron loss in order to provide efficient electrical devices such as transformers and rotating machines. Scanning electron microscope (SEM) makes it possible to observe domain structures using electrical steel sheets (the thickness is mostly 10^{-4} m order) in practical use. On the other hand, it is difficult to carry out the real time observation. Moreover, any dynamic observation techniques are basically impossible to obtain the domain images continuously in time or applied field axes even if the real time observation. Thereby, the continuous macroscopic/microscopic hysteresis loops are not obtained by domain observation. The aim of this study is to obtain continuous macroscopic/microscopic magnetization curves from discretely given domain images.

This paper proposes a method of magnetization curve plotting from a series of the distinct grain-oriented electrical steel SEM domain images. Instead of measuring enormous number of images, we employ the images Helmholtz equation method [3] which makes it possible to extract parameters characterizing transition information of animation from its frames. As a result

of computation using these parameters makes it possible to generate animation continuously.

The macroscopic magnetization curve is computed from the contrasts of magnetized domain images generated by the image Helmholtz equation, which describes the magnetization characteristics at the particular points on the domain image. The microscopic magnetization curves are obtained from the pixel values, constructing the digital image, at a position of the generated domain images as well.

II. IMAGE HELMHOLTZ EQUATION

A. Domain Images of a Grain-Oriented Electrical Steel

Fig. 1 shows the domain images of a grain-oriented electrical steel under the distinct magnetized states [4]. The specimen is the ORIENTCORE·HI-B (Nippon Steel Corporation product) without surface coating and its thickness is 0.23 mm. The observation of backscattered electrons was carried out using SEM at 160 keV [5]. The conditions of domain images used in this paper are listed in Table I.

B. Image Helmholtz Equation

To obtain continuous magnetization curves, we employ the image Helmholtz equation method to given domain images [3]. Suppose that a domain image is composed of a scalar field U, and then the dynamics of magnetic domains can be represented by the image Helmholtz equation. In magnetized state, the domain motion is caused by external magnetic field H, so that our image Helmholtz equation is reduced into:

$$\nabla^2 U + \varepsilon \frac{\partial}{\partial H} U = -\sigma \tag{1}$$

where ε and σ respectively denote a domain motion parameter and an image source density given by the Laplacian of final image U_{Final} [6]. The first and second terms on the left in (1) mean the spatial expanse and transition of image to the variable H, respectively. The parameter ε in (1) is not given. Key idea of our method is to determine the ε from given SEM images.

C. Solution of the Image Helmholtz Equation

The modal analysis to (1) gives a general solution [3]:

$$U(H) = \exp(-\Lambda H)(U_{Start} - U_{Final}) + U_{Final} \tag{2}$$

where U_{Start} and $\exp(-\Lambda H)$ are an initial image and a state transition matrix, respectively. Because of the parameter ε in (1), the state transition matrix is unknown. It is essentially required to determine the state transition matrix from the given domain images.

H. Endo, S. Hayano, and Y. Saito are with the Graduate School of Engineering, HOSEI University, 3-7-2 Kajino, Koganei, Tokyo 184-8584, Japan (e-mail: endo@ysaitoh.k.hosei.ac.jp).

M. Fujikura and C. Kaido are with the Technical Development Bureau, Nippon Steel Corporation, 20-1 Shintomi, Futtsu, Chiba 293-8511, Japan (e-mail: m-fujikura@lab.re.nsc.co.jp).
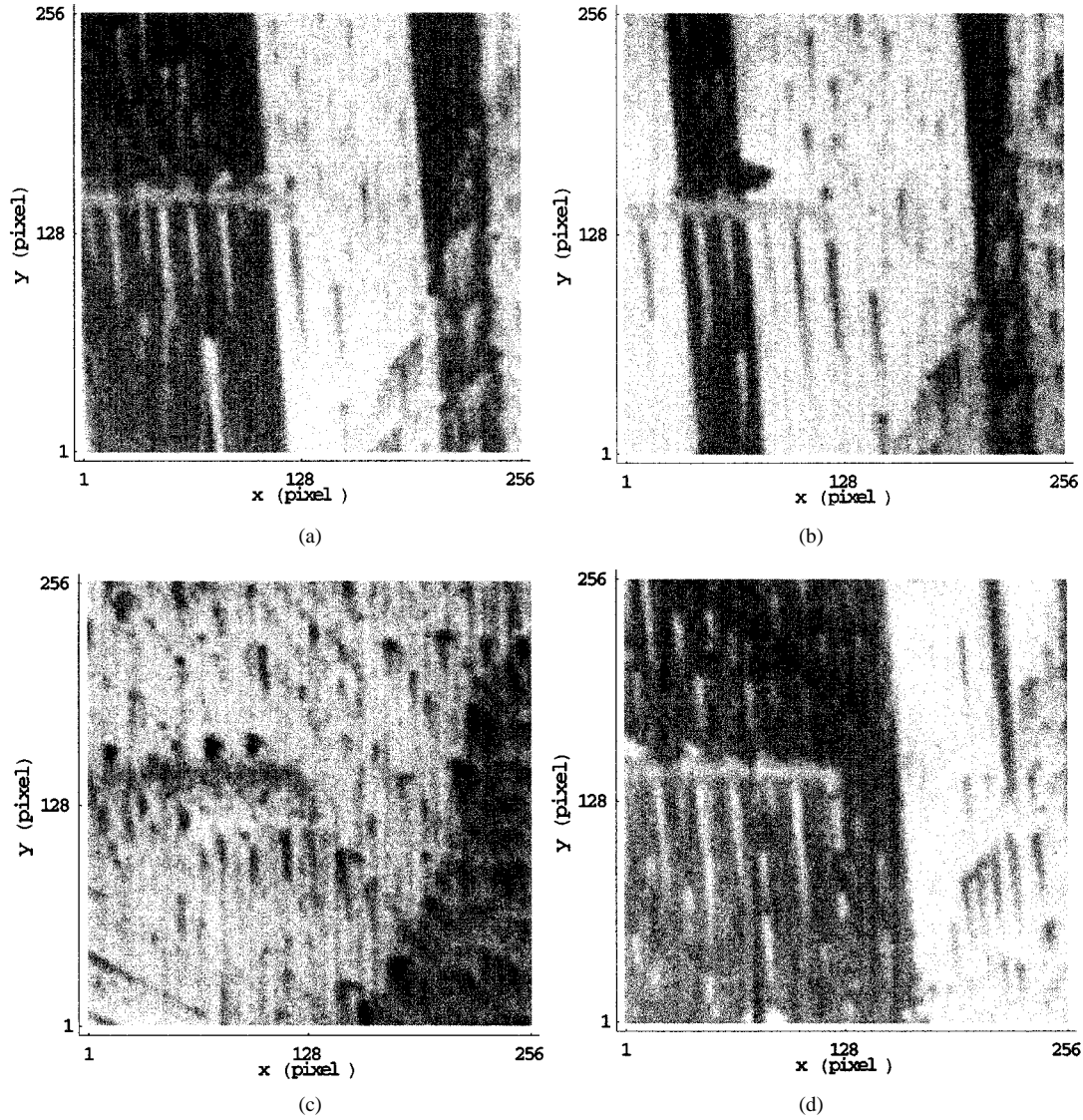
(a)

(b)

(c)

(d)

Fig. 1. Magnetic domain images of a grain-oriented electrical steel observed by SEM (256×256 pixels, 0.01 mm/pixel). (a)–(d) are the domain images numbered as 1, 3, 11, and 19 in Table I, respectively. The y-direction is the rolling direction and applied field axis.

D. Determination of the State Transition Matrix

If we have the solution $U(H)$ in (2), then it is possible to determine the elements in matrix Λ by modifying (2), as given by

$$\Lambda = -\frac{1}{H} \ln \left(\frac{U(H) - U_{Final}}{U_{Start} - U_{Final}} \right). \tag{3}$$

Thereby, the elements in the ith matrix Λ_i is determined from a series of three distinct domain images by means of (4).

$$\Lambda_i = -\frac{1}{H_{i+1} - H_i} \ln \left(\frac{U_{i+1} - U_{i+2}}{U_i - U_{i+2}} \right),$$
$$i = 1, 2, \ldots, 22. \tag{4}$$

The subscript i refers to a domain image numbered in Table I. The domain images U_i and U_{i+2} correspond to U_{Start} and

TABLE I
CONDITIONS OF MEASURED DOMAIN IMAGES H: EXTERNAL MAGNETIC FIELD
INTENSITY, B: FLUX DENSITY

Image No.	H(A/m)	B(T)	Image No.	H(A/m)	B(T)
1	0.00	0.00	13	214.13	1.93
2	2.85	0.10	14	160.37	1.92
3	9.26	1.63	15	98.68	1.91
4	24.16	1.73	16	54.66	1.84
5	30.23	1.78	17	28.53	1.83
6	54.59	1.84	18	3.73	1.77
7	84.92	1.86	19	0.00	1.73
8	115.39	1.88	20	-4.60	1.73
9	160.69	1.90	21	-5.95	-0.06
10	236.32	1.92	22	-7.45	-1.43
11	324.31	1.95	23	-9.07	-1.56
12	269.64	1.95	24	-11.50	-1.62

U_{Final} in (2), respectively. It is possible to analytically generate a domain image by substituting Λ_i into (2).
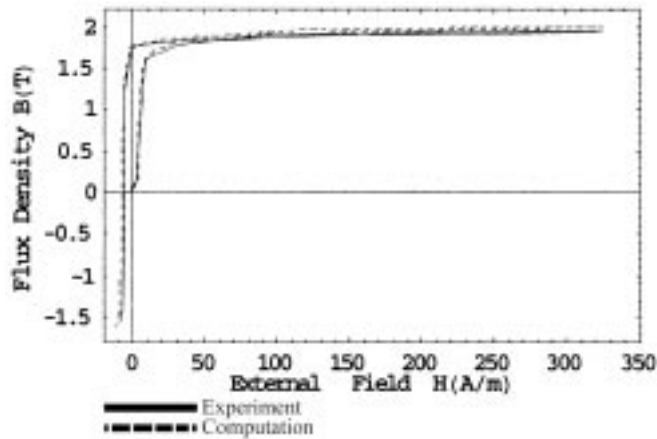
Fig. 2. Macroscopic magnetization curve reconstruction.

E. Physical Meaning of the Matrix Λ

According to Preisach model, the relationship between the magnetic field and flux density can be represented by

$$\frac{1}{\mu}B + \frac{1}{\Psi}\frac{\partial B}{\partial(H_{\text{eff}} - H_c)} = H_{\text{eff}} - H_c \qquad (5)$$

where H_{eff} and H_c represent the effective and coercive fields, respectively. Moreover, Ψ denotes the Preisach distribution function [7]–[9]. Comparing ε in (1) and Ψ in (5), the matrix Λ_i obtained by (4) are a reciprocal of the Preisach distribution function. The Preisach function is a rate of change of permeability to the external field H. Thereby, our method fully takes into account the magnetic hysteresis. Since the elements in the matrix Λ should be constant values, then this approximation is only satisfied in small dB/dH region.

III. MAGNETIZATION CURVES PLOTTING

A. Macroscopic Magnetization Curve

The contrast of SEM images shown in Fig. 1 means the polarity of magnetization. A summation of all magnetization gives a flux density in a magnetic material. Computing an average of pixel values of an entire domain image just corresponds to a flux density in a magnetic material.

Fig. 2 shows the computed magnetization curve. Since (2) is possible to generate the domain images analytically, then the smooth computed magnetization curve is generated. Even though the domain images represent a limited area of the specimen, we have good agreement with the experimental result as shown in Fig. 2.

B. Microscopic Magnetization Curves

When we focus on a magnetization curve at a particular point on the domain image, it is possible to draw the microscopic magnetization curves. In order to demonstrate the microscopic magnetization curves, Fig. 3 shows the selected sample positions depending on the physical differences. The features of the selected positions in Fig. 3 are as follows.

- Position Nos. 1 and 2: At the 180° domains
- Position Nos. 3 and 4: At the lancet domains
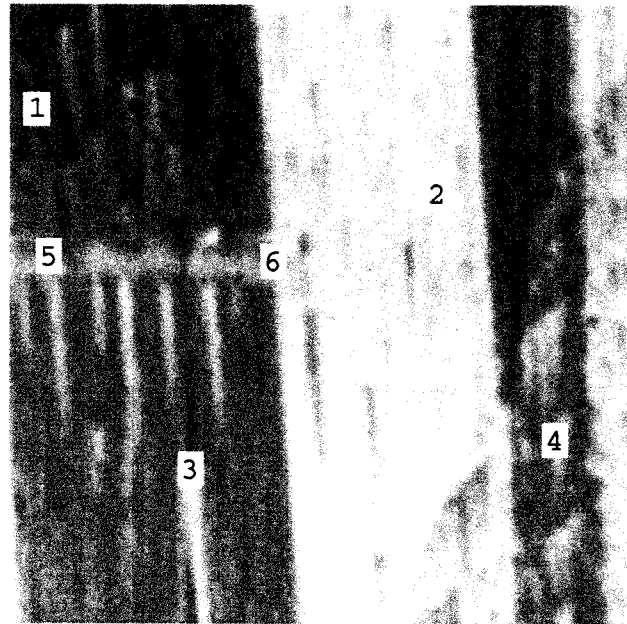- Position Nos. 5 and 6: At the strained parts.

Fig. 3. Selected pixel positions for drawing the microscopic magnetization curves. The background domain image is the same one as Fig. 1(a). The positions 1 and 2 are at the 180° domains. The positions 3 and 4 are at the lancet domains. The positions 5 and 6 are at the strained parts.
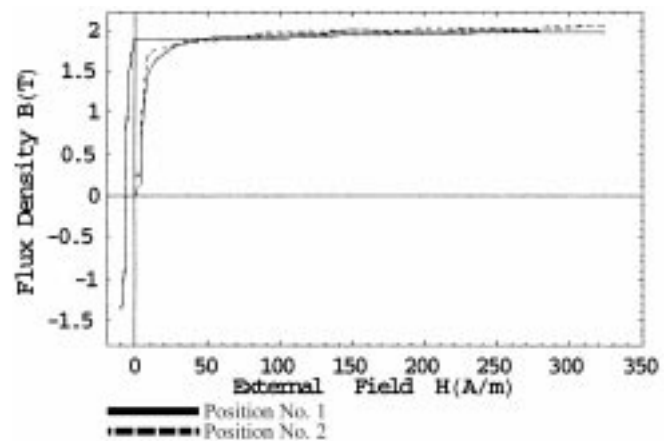

Fig. 4. Magnetization curves at the 180° domains in Fig. 3.

Figs. 4–6 show the magnetization curves computed from each of the pixel values. At first, in the magnetization curves at the 180° basic domains (Fig. 4), the residual inductions are higher than those at the lancet domains (Fig. 5) and the strained parts (Fig. 6). This means that the lancet and strained parts are hard to be magnetized. Inversely, the 180° basic domains are hard to move due to keeping minimum static magnetic energy. Second, in Fig. 5, the discontinuous curves are obtained at the beginning of rotating magnetization region due to the lancet domain generations. This results in supporting [10]. Finally, in Fig. 6, a discontinuous curve is obtained at the position 5 due to the physical stress to the specimen. However, the curve at the position 6 is reconstructed smoothly. This is considered to cause by stretching strain.
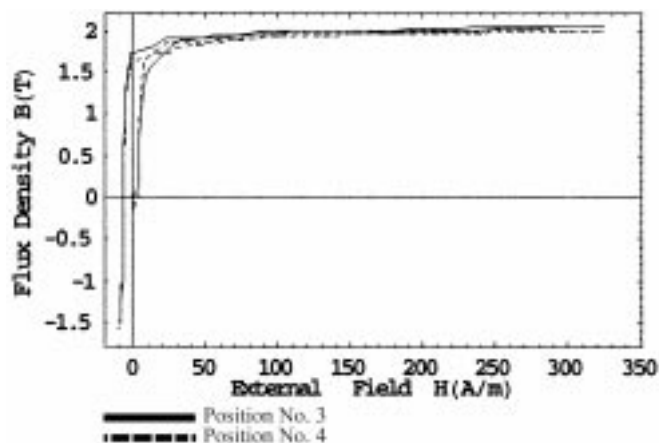
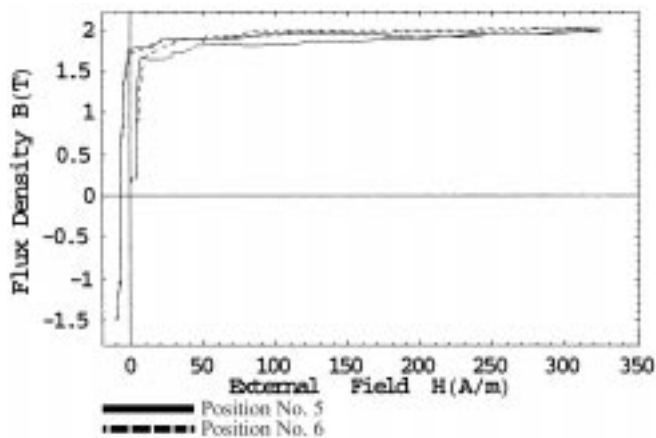Fig. 5.   Magnetization curves at the lancet domains in Fig. 3.

Fig. 6.   Magnetization curves at the strained parts in Fig. 3.

IV. Conclusions

We have proposed the magnetization curves drawing from a series of the distinct magnetized domain images. Instead of the real time observation, domain motion information is deduced from the parameters determined by means of image Helmholtz equation. Even though only a small number of images are given, the macroscopic/microscopic magnetization curves can be generated reflecting on the domain physical situations by our method. This methodology is not only applicable to more smaller or larger scale domain images but also another kinds of imaging techniques.

References

[1] J.-P. Jamet *et al.*, "Dynamics of the magnetization reversal in Au/Co/Au micrometer-size dot arrays," *Phys. Rev. B*, vol. 57, no. 22, pp. 14 320–14 331, 1998.

[2] S.-B. Choe and S.-C. Shin, "Magnetization reversal dynamics with sub-micron-scale coercivity variation in ferromagnetic films," *Phys. Rev. B*, vol. 62, no. 13, pp. 8646–8649, 2000.

[3] H. Endo, S. Hayano, Y. Saito, and T. L. Kunii, "A method of image processing and its application to magnetodynamic fields," *Trans. IEE of Japan (in Japanese)*, vol. 120-A, no. 10, pp. 913–918, 2000.

[4] T. Nozawa, T. Yamamoto, Y. Matsuo, and Y. Ohya, "Effects of scratching on losses in 3-percent Si–Fe single crystals with orientation near (110)[001]," *IEEE Trans. Magn.*, vol. 15, no. 2, pp. 972–981, 1979.

[5] A. Hubert and R. Schäfer, *Magnetic Domains*.   Berlin: Springer, 2000.

[6] H. Endo, S. Hayano, Y. Saito, and T. L. Kunii, "Image governing equations and its application to vector fields," *Trans. IEE of Japan (in Japanese)*, vol. 120-A, no. 12, pp. 1089–1094, 2000.

[7] L. Liorzou, B. Phelps, and D. L. Atherton, "Macroscopic models of magnetization," *IEEE Trans. Magn.*, vol. 36, no. 2, pp. 418–427, 2000.

[8] Y. Saito, S. Hayano, and Y. Sakaki, "A parameter representing eddy current loss of soft magnetic materials and its constitutive equation," *J. Appl. Phys.*, vol. 64, no. 1, pp. 5684–5686, 1988.

[9] Y. Saito, K. Fukushima, S. Hayano, and N. Tsuya, "Application of a Chua type model to the loss and skin effect calculation," *IEEE Trans. Magn.*, vol. 23, no. 5, pp. 2227–2229, 1987.

[10] C. Kaido *et al.*, "A discussion of the magnetic properties of nonoriented steel sheets," in *Workshop of IEE of Japan, (in Japanese)*, 1999, MAG-99-173.